

Size dependent decay of the surface plasmon excitation in gold nanoparticles

C. Hendrich,* F. Hubenthal, and F. Träger

Institut für Physik and Center for Interdisciplinary Nanostructure Science and Technology - CINSaT,

Universität Kassel, Heinrich-Plett-Strasse 40, D-34132 Kassel, Germany

(Dated: March 19, 2005)

The ultrafast electron dynamics in gold nanoparticles has been studied by measuring the dephasing time T_2 of the surface plasmon polariton as a function of particle size and plasmon energy. Persistent spectral hole burning which permits to overcome the inhomogeneous broadening caused by the size and shape distributions, has been applied to oblate gold nanoparticles on sapphire substrates. Dephasing times ranging from 5 to 17 fs were extracted and an increased damping at higher plasmon energies due to an interband transition was observed. Furthermore, an explicit influence of the reduced dimensions of the nanoparticles was detected. A value of $T_2 = 5.6$ fs for a particle radius of 3.7 nm was extracted. Comparison with other measurements as well as with theoretical predictions could identify surface scattering and for the first time size dependent Landau-damping as the most dominant damping mechanisms.

PACS numbers: Valid PACS appear here

I. INTRODUCTION

Metal nanoparticles are one of the most promising nanoscale materials for future applications [1]. They exhibit many new properties which are unknown for the bulk material and which depend strongly on the particle dimensions in nearly all cases. For example size dependent alloying [2], melting point [3], catalytic reactivity [4], electronic [5–7] and optical properties [8, 9] have been examined in the past.

Especially the optical properties of metal nanoparticles distinguish clearly from those of the bulk material, because they are dominated by the surface plasmon polaritons (SPP). These are coherent oscillations of the conduction band electrons against the ion cores which can be excited by light [9]. Investigation of the spectral positions and line widths of the resonances allows therefore to probe the electronic properties of the particles, e.g. confinement of electronic states [10].

The linear optical properties of metal nanoparticles were studied extensively in the last decades, mostly focussing on the influence of particle material, size, shape and dielectric surrounding on the amplitude and energy

*Present address: Laboratory of solid state physics and magnetism, K.U. Leuven, Celestijnenlaan 200D, B-3001 Leuven, Belgium; Electronic address: hendrich@physik.uni-kassel.de

of the SPP [8]. Contrary to this, only few experiments examined the decay of the SPP, which takes part within only several femtoseconds after excitation [11–16]. The characteristic time for the decoherence of the electronic oscillation is the dephasing time T_2 , which can be determined from the homogeneous line width of the SPP resonance and is an adequate gauge for the dephasing processes.

With the knowledge of the dephasing of the SPP, local field enhancement near the nanoparticles' surface can be optimized [17, 18]. This effect is accompanied with the SPP and can be used for optical tweezers [19], to enhance the Raman-scattering of molecules [20, 21] or to improve the resolution in fluorescence microscopy [22]. The dephasing time T_2 is the key parameter for these applications because it is predicted to be directly proportional to the enhancement factor of the local field [Zitat für Proportionalität bitte Matthias fragen].

II. THE DECAY OF THE SURFACE PLASMON

Theoretically, the decay of the SPP results from the coaction of different processes which are discussed widely in literature [23–27]. For particles with $1.5 \text{ nm} < R < 25 \text{ nm}$ and low intensities of the incident electromagnetic field several damping mechanisms, e.g. emission of electrons [24] and radiation damping [28] can be neglected. On the time scale smaller than 20 fs after plasmon excitation only three effects play a role [??]:

Surface scattering is the inelastic scattering of the co-

herent oscillating electrons at the particle surface. It gets relevant as soon as the nanoparticle radius is smaller than the free path of the electrons l_∞ at the Fermi edge. The damping is determined by the Fermi velocity v_F divided by the particle radius, i.e. $1/T_2 \propto v_F/R$. This correlation is predicted theoretically [7, 29] and observed in a few experiments [13, 15, 30].

Landau-damping describes the resonant generation of electron-hole-pairs [25, 26, 31]. In contrast to surface scattering, it is a collisionless damping, because electron-electron interactions are mostly not involved. Depending on the photon energy, intra- and interband-transitions are contributing [32]. Moreover, the amount of Landau-damping is proportional to the surface to volume ratio of the particle, i.e. a $1/R$ -dependence of $1/T_2$ is predicted [6, 24, 33]. This is due to the broadening of the discrete eigenstates of the holes and quasifree electrons which are determined by the particles surface [10].

Chemical interface damping (CID) is the dynamic tunneling of the oscillating electrons into and out of adsorbate or surface states. Due to the statistic nature of the tunneling, the electrons lose the phase coherence which results in additional damping [7, 15, 16, 34]. Because of the surface-sensitivity, a $1/R$ -dependence is predicted.

All three effects predict a $1/R$ -dependence of the inverse dephasing time which can be taken into account by

$$1/T_2 = 1/T_{2,\infty} + \sum_i A_i/R, \quad (1)$$

where A_i are the corresponding damping parameters which describe the size dependence of each contribution [8]. The dephasing time $T_{2,\infty}$ which is expected for the bulk material depends on the SPP energy $\hbar\Omega$ and can be calculated by the Drude model using the dielectric constants ϵ_1, ϵ_2 of the nanoparticle material [8, 35]:

$$T_{2,\infty}(\Omega) = \left| \frac{d\epsilon_1(\omega)}{d\omega} \Big|_{\omega=\Omega} \right| / \epsilon_2(\Omega). \quad (2)$$

III. PREPARATION AND CHARACTERIZATION

Gold atoms from a thermal atom beam were deposited on sapphire surfaces under ultrahigh vacuum conditions. By diffusion and subsequent nucleation at defect sites on the substrate, oblate nanoparticles were grown, a process known as Volmer-Weber-growth [36]. The shapes of the nanoparticles were approximated by rotational ellipsoids with the short axis a perpendicular and the long axis b parallel to the surface. The axial ratio a/b , the equivalent radius R_{eq} , which is the radius of a sphere with the same volume and the size distribution of the ensemble were used to characterize the nanoparticles. Furthermore, the axial ratio of the nanoparticles depends definitely on their size, an effect that is caused by the growth mechanism [37].

The optical properties of ellipsoidal particles are domi-

nated by two SPP modes: The (1,0)- and the (1,1)-mode, i.e. the electronic excitation parallel to the long axis and the short axis respectively. With p-polarized light and under an angle of incidence different from normal incidence, both SPP modes and with s-polarized light only the (1,1)-mode can be excited. Nevertheless, for gold nanoparticles, the (1,0)-mode is suppressed by the impact of an interband transition located at about 2.4 eV [38, 39]. An important issue is that the spectral positions of the SPR only depend on the axial ratio and not on the size, if radii of $1 \text{ nm} < 20 \text{ nm}$ are considered. Therefore the axial ratios of the nanoparticles can be calculated by modeling the extinction spectra with quasistatic approximation [9]. The radii of the nanoparticles were calculated from the amount of deposited material and the particle number density which was determined by atomic force microscopy [37].

IV. METHOD OF PERSISTENT SPECTRAL HOLE BURNING

Spectral hole burning is based on selective size and shape modification of nanoparticles with laser light [15, 40–42]. In short, the nanoparticle ensembles are irradiated with nanosecond laser pulses whose photon energy falls within the inhomogeneously broadened absorption profile. Only resonant particles absorb the laser light efficiently and convert it into heat (Fig. 1a). Thus diffusion and desorption of atoms at the surface of these particles are initialized. While diffusion only alters the shape to-

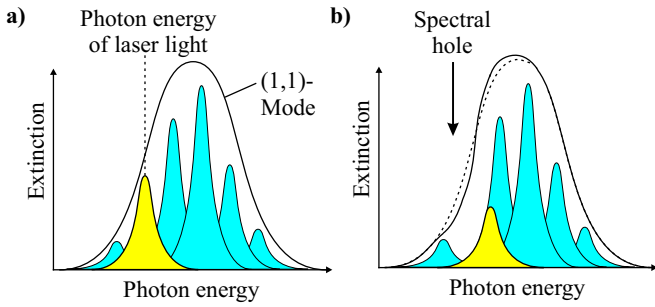


FIG. 1: Schematic illustration of the spectral hole burning process. a) Only resonant nanoparticles absorb the nanosecond laser pulses and are selectively heated. b) The SPR of the reshaped particles is shifted to higher energies and its amplitude is decreased. In the overall spectrum a spectral hole is burned.

wards a sphere, the desorption also reduces the particle volume. As a consequence the SPR of the resonant particles is shifted to higher photon energies and its extinction is decreased (Fig. 1b). In the overall spectrum a hole is burned at the photon energy of the laser light and an increase of extinction occurs at higher photon energies due to the modified particles. The width of these spectral holes increases linearly with growing laser fluence because also non-resonant particles absorb the laser light in the wings of their SPR, an effect called power broadening. The laser induced modifications were modeled theoretically, whereas the spectral changes due to desorption and diffusion as well as the power broadening effect were taken into account [15, 35, 43]. The homogeneous line width Γ_{hom} was obtained by linear extrapolation of the hole widths to vanishing laser fluences [30, 41, 44]. The dephasing time T_2 was finally determined by using the

uncertainty relation $T_2 = 2\hbar/\Gamma_{\text{hom}}$.

V. EXPERIMENTAL

All experiments were carried out under ultrahigh vacuum conditions ($p < 10^{-8}$ mbar). A thermal beam of gold atoms was generated by an electron beam evaporator and directed onto sapphire substrates, on which the nanoparticles were formed by Volmer-Weber-growth. Atomic force microscopy in the ultrahigh vacuum as well as under ambient conditions was used to determine the number density of the nanoparticles on the substrates. The optical spectra were recorded under an angle of incidence of 45° using the s-polarized light from a xenon arc lamp in combination with a monochromator. For spectral hole burning the samples were cooled down to 100 K and subsequently nanosecond laser pulses (pulse length 5-7 ns, repetition rate 10 Hz) with different photon energies and fluences were applied. The laser light was generated with a BBO-OPO (beta-barium-borate optical parametric oscillator) which was pumped by the third harmonic of a Nd:YAG laser. The angle of incidence of the laser light was set perpendicular to the substrate surface and the polarisation was the same as chosen for the extinction measurements. The beam was focussed down to a diameter of 1.5 mm utilizing a quartz lens. In order to modify a significant amount of nanoparticles on the substrates, the beam was scanned over the sample surface.

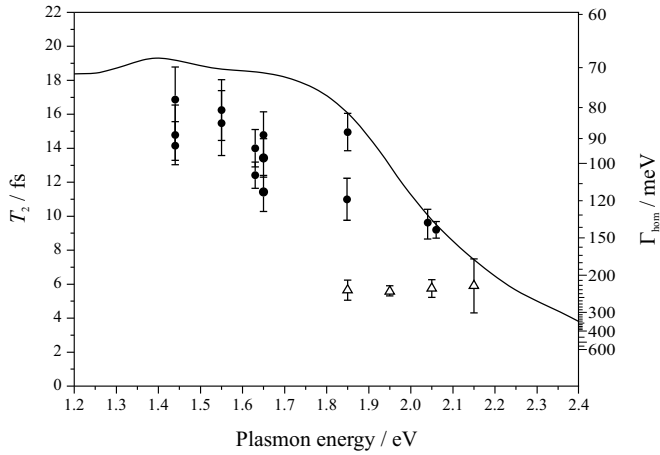


FIG. 2: Dephasing time (left axis) and homogeneous line width (right axis) of the SPP as a function of plasmon energy. Filled circles: particles with radii of 9-15 nm, open triangles: particles with radii of 4-6 nm. The solid line was obtained by using eq. (2) with the bulk dielectric function from [39].

VI. DEPENDENCE OF THE DEPHASING TIME ON THE PLASMON ENERGY

The dephasing time of the SPP was measured as a function of the plasmon energy (Fig. 2). The equivalent radii ranged from 9 to 15 nm and the axial ratios of the nanoparticles increased with rising photon energies from 0.06 to 0.26 (filled circles). The dephasing times decrease from 15 fs at a photon energy of 1.44 eV to a value of only 9 fs at 2.05 eV, i.e. an increasing damping of the SPP is observed at higher plasmon energies. This decrease of T_2 is due to the impact of an interband transition from the d-band into the conduction band which is located at about 2.4 eV [8, 38]. The solid line was calculated using the dielectric function ϵ_{bulk} of bulk gold [39] using eq. (2) and refers to T_2 assuming the nanoparticles to have the

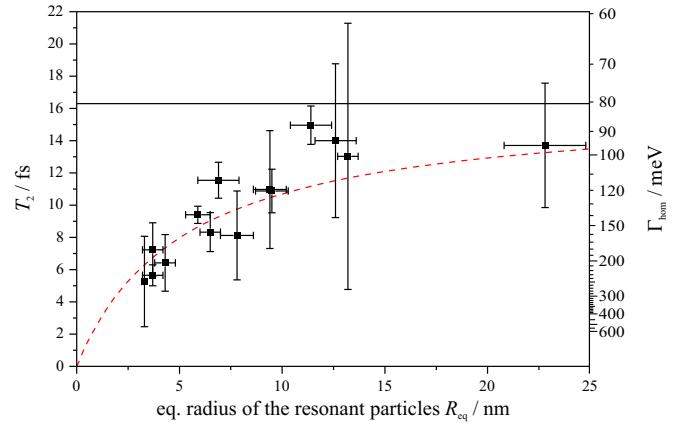


FIG. 3: Dephasing time (left axis) and homogeneous line width (right axis) as a function of the equivalent radius of the gold nanoparticles. The solid line represents the dephasing time of $T_2 = 16.3$ fs calculated from ϵ_{bulk} and the dashed line a fit of the $1/R_{\text{eq}}$ -dependence from eq. (1) which is predicted by several models.

electronic properties of gold bulk.

VII. DEPENDENCE OF THE DEPHASING TIME ON THE NANOPARTICLE SIZE

The influence of the reduced dimension on the dephasing time was investigated by measuring T_2 of very small nanoparticles with radii of only 4-6 nm (Fig. 2, open triangles). Much shorter dephasing times of about 5.5 fs were extracted, which is a clear evidence for size dependent effects.

To identify these contributing size dependent damping mechanisms, the shortening of T_2 for small nanoparticles was investigated in more detail by varying the nanoparticle size at a fixed plasmon energy. For this purpose, nanoparticles with different sizes and constant shape were

prepared: Large particles with higher axial ratios than usual were generated with the technique of laser-assisted growth [45, 46] and small nanoparticles with a more oblate shape were grown at low temperatures ($T = 100$ K). Thus, the mean axial ratio and the SPR could be kept constant independently of the particle size. The laser photon energy used for hole burning was set to 1.85 eV, being located within the inhomogeneous broadened SPR. For this plasmon energy we expect Landau-damping as well as surface scattering to contribute to the size-dependence of T_2 . Nanoparticles with radii ranging from 3 to 23 nm and an axial ratio of $a/b = 0.13$ were examined. The results are shown in Fig. 3. While the experimentally determined dephasing times for the particles with radii above 12 nm are only slightly lower than the value obtained from the dielectric function of the gold bulk [7], T_2 decreases significantly for smaller nanoparticles and reaches a value of only (5.6 ± 0.7) fs for a radius of (3.7 ± 0.5) nm. This clearly shows the influence of the reduced dimension on the damping of the SPP. Therefore eq. (1) was fitted to the experimental data (Fig. 3, dashed line) by using A as fit parameter and $T_{2,\infty} = 16.3$ fs. A value of $A = (0.32 \pm 0.06)$ nm/fs was obtained, which describes the increase of the T_2 with declining particle size.

VIII. DISCUSSION

First, the results of the measurements varying the plasmon energy, i.e. the particle shape are discussed. Two

different contributions to the dephasing of the SPP are found (Fig. 2): Above 1.85 eV the Landau-damping by the interband transition is the dominant damping mechanism and the experimental data converge against the values calculated from the bulk dielectric function. For plasmon energies below 1.85 eV, the measured dephasing times lie significantly below the values from ϵ_{bulk} . Nevertheless, in this range the influence of the interband transition is neglectable and chemical interface damping can be excluded because it is found to be not important for gold and silver nanoparticles on sapphire substrates [15, 41]. Therefore the low values of T_2 are ascribed to surface scattering [41]. In summary, already for these large nanoparticles with radii of 9-15 nm an explicit influence of their reduced dimension on the electronic properties is found.

Below, the dependence of T_2 on the particle size (Fig. 3) is discussed. The measured damping parameter A was obtained at a SPP energy of 1.85 eV where the influence of both damping mechanisms mentioned above is expected. Our value is significantly higher than $A_{\text{Persson}} = 0.2$ nm/fs, which is calculated for pure surface scattering using the equations of Persson [7]. This indicates the presence of Landau-damping that is predicted to get dominant for Plasmon energies above 1.8 eV [6, 13]. Thus, we attribute these increased size dependent damping of $\Delta A \approx 0.12$ nm/fs to Landau-damping.

Our results are also in good agreement with other measurements made for gold nanoparticles on quartz sub-

strates at a plasmon energy of 2.3 eV [13]. In these measurements a value of $A_{\text{Dalacu}} = 0.31$ nm/fs was extracted from only four data points. A_{Dalacu} is close our A -parameter, but not directly comparable, because of the different plasmon energy. An influence on the dephasing time from the quartz substrate which was used in these experiments can not be excluded [15].

IX. CONCLUSIONS

To our knowledge, the *size dependent* influence of Landau-damping of the SPP could be separated for the first time from the effect of surface scattering. By measuring the dephasing time T_2 with the technique of spec-

tral hole burning, a clear dependence on the inverse particle radius of was found. Variation of the energy of the SPP showed that below 1.85 eV only surface scattering is observed while for higher plasmon energies also Landau damping contributes to the size dependent damping process.

Acknowledgements

Financial support by the Deutsche Forschungsgemeinschaft and the Fonds der Chemischen Industrie is gratefully acknowledged. C.H. is also grateful to the Kasseler Hochschulbund.

-
- [1] V. Rotello, ed., *Nanoparticles: Building Blocks for Nanotechnology*, Nanostructure Science and Technology (Kluwer Academic/Plenum Publishers, New York, 2004).
- [2] H. G. Boyen, A. Ethirajan, G. Kästle, F. Weigl, P. Ziemann, G. Schmid, M. G. Garnier, M. Buttner, and P. Oelhafen, *Phys. Rev. Lett.* **94**, 016804 (2005).
- [3] K. Koga, T. Ikeshoji, and K. Sugawara, *Phys. Rev. Lett.* **92**, 115507 (2004).
- [4] U. Heiz, A. Sanchez, S. Abbet, and W.-D. Schneider, *J. Am. Chem. Soc.* **121**, 3214 (1999).
- [5] U. Kreibig, *J. Phys. F* **4**, 999 (1974).
- [6] C. Yannouleas and R. A. Broglia, *Ann. Phys.* **217**, 105 (1992).
- [7] B. N. J. Persson, *Surf. Sci.* **281**, 153 (1993).
- [8] U. Kreibig and M. Vollmer, *Optical Properties of Metal Clusters* (Springer, Berlin, 1995).
- [9] C. F. Bohren and D. R. Huffman, *Absorption and Scattering of Light by Small Particles* (Wiley, New York, 1983).
- [10] A. Kawabata and R. Kubo, *J. Phys. Soc. Japan* **21**, 1765 (1966).
- [11] B. Lamprecht, A. Leitner, and F. R. Aussenegg, *Appl. Phys. B* **68**, 419 (1999).
- [12] C. Sönnichsen, T. Franzl, T. Wilk, G. von Plessen, J. Feldmann, O. Wilson, and P. Mulvaney, *Phys. Rev. Lett.* **88**, 077402 (2002).
- [13] D. Dalacu and L. Martinu, *J. Opt. Soc. Am. B* **18**, 85 (2001).
- [14] N. Nilius, N. Ernst, and H.-J. Freund, *Phys. Rev. B* **65**, 115421 (2002).
- [15] J. Bosbach, C. Hendrich, F. Stietz, T. Vartanyan, and F. Träger, *Phys. Rev. Lett.* **89**, 257404 (2002).
- [16] C. Hendrich, J. Bosbach, F. Stietz, F. Hubenthal, T. Var-

- tanyan, and F. Träger, Appl. Phys. B **76**, 869 (2003).
- [17] A. Wokaun, Mol. Phys. **56**, 1 (1985).
- [18] P. W. Barber, R. K. Chang, and H. Massoudi, Phys. Rev. Lett. **50**, 997 (1983).
- [19] L. Novotny, R. X. Bian, and X. S. Xie, Phys. Rev. Lett. **79**, 645 (1997).
- [20] K. Sokolov, G. Chumanov, and M. Cotton, Anal. Chem. **70**, 3898 (1998).
- [21] S. Nie and S. R. Emory, Science **275**, 1102 (1997).
- [22] M. Alschinger, M. Maniak, F. Stietz, T. Vartanyan, and F. Träger, Appl. Phys. B **76**, 771 (2003).
- [23] J.-Y. Bigot, V. Halté, J.-C. Merle, and A. Daunois, Chem. Phys. **251**, 181 (2000).
- [24] F. Calvayrac, P. G. Reinhard, E. Suraud, and C. A. Ullrich, Phys. Rep. **337**, 493 (2000).
- [25] P.-G. Reinhard, M. Brack, F. Calvayrac, C. Kohl, S. Kömmel, E. Suraud, and C. A. Ullrich, Eur. Phys. J. D **9**, 111 (1999).
- [26] H.-G. Rubahn, Appl. Surf. Sci. **109/110**, 575 (1997).
- [27] E. J. Heilweil and R. M. Hochstrasser, J. Chem. Phys. **82**, 4762 (1985).
- [28] J. Crowell and R. H. Ritchie, Phys. Rev. **172**, 436 (1968).
- [29] U. Kreibig and L. Genzel, Surf. Sci. **156**, 678 (1985).
- [30] F. Hubenthal, T. Ziegler, C. Hendrich, T. Vartanyan, and F. Träger, Proc. SPIE **5221**, 29 (2003).
- [31] D. Pines and P. Nozières, *The Theory of Quantum Liquids* (Benjamin, New-York, 1966).
- [32] S. A. Maier, P. G. Kika, H. A. Atwater, S. Meltzer, A. A. G. Requicha, and B. E. Koel, Proc. SPIE **4810** (2002).
- [33] V. O. Nesterenko, W. Kleinig, and P.-G. Reinhard, Eur. Phys. J. D **19**, 57 (2002).
- [34] A. Hilger, M. Tenfelde, and U. Kreibig, Appl. Phys. B **73**, 361 (2001).
- [35] T. Vartanyan, J. Bosbach, F. Stietz, and F. Träger, Appl. Phys. B **73**, 291 (2001).
- [36] M. Volmer and A. Weber, Z. Phys. Chem. **119**, 277 (1925).
- [37] T. Wenzel, J. Bosbach, F. Stietz, and F. Träger, Surf. Sci. **432**, 257 (1999).
- [38] R. Lässer and N. V. Smith, Solid State Commun. **37**, 507 (1981).
- [39] P. B. Johnson and R. W. Christy, Phys. Rev. B **6**, 4370 (1972).
- [40] J. Bosbach, C. Hendrich, T. Vartanyan, F. Stietz, and F. Träger, Euro. Phys. J. D **16**, 213 (2001).
- [41] C. Hendrich, T. Ziegler, J. Bosbach, T. Vartanyan, F. Hubenthal, and F. Träger, Proc. SPIE **5352** (2004).
- [42] F. Stietz, J. Bosbach, T. Wenzel, T. Vartanyan, A. Goldmann, and F. Träger, Phys. Rev. Lett. **84**, 5644 (2000).
- [43] T. Vartanyan, J. Bosbach, C. Hendrich, F. Stietz, and F. Träger, Proc. SPIE **4636**, 31 (2002).
- [44] T. Ziegler, C. Hendrich, F. Hubenthal, T. Vartanyan, and F. Träger, Chem. Phys. Lett. **386**, 319 (2004).
- [45] F. Hubenthal, C. Hendrich, H. Ouacha, D. B. Sanchez, and F. Träger, Euro. Phys. J. D (2004).
- [46] T. Wenzel, J. Bosbach, A. Goldmann, F. Stietz, and F. Träger, Appl. Phys. B **69**, 513 (1999).